05,13

Features of the manifestation of antiferromagnetism of the Cr-Mn alloy in the film composites of the (Cr-Mn)/Fe type

© A.A. Feshchenko[1], M.E. Moskalev[1], A.N. Gorkovenko[1], V.N. Lepalovskij[1], E.A. Stepanova[1], E.A. Kravtsov[1,2], V.O. Vas'kovskiy[1,2]

[1] Ural Federal University,
Ekaterinburg, Russia
[2] Institute of Metal Physics, UB RAS,
Ekaterinburg, Russia

E-mail: a.a.feshchenko@urfu.ru

Received April 17, 2023
Revised April 17, 2023
Accepted May 11, 2023

This paper presents a detailed study of the hysteresis properties of film structures based on bilayers of the Cr-Mn/Fe type. The temperature dependences of several parameters of the hysteresis loops of the Fe layers are determined for films varying in the composition and thickness of the Cr-Mn layer, as well as in the structure of buffer coatings. The compositional and temperature intervals of the existence of the antiferromagnetic ordering in the Cr-Mn layer and the related features of the temperature changes in the coercive force, its anisotropy in the plane of the films and the exchange bias field are established. The causal analysis of the established regularities is performed.

Keywords: antiferromagnet, ferromagnet, bilayers, thickness, composition, temperature, texture, coercive force, exchange bias.

DOI: 10.21883/PSS.2023.06.56102.09H

1. Introduction

Cr-Mn binary alloy belongs to the group of high-temperature antiferromagnetics [1] and in this regard is of interest for spintronics devices, in particular spin valves, as a source of magnetic fixation in layered film structures of ferromagnetic/antiferromagnetic [2–4] type. However, it is poorly researched as such. And in general, there is little information in the literature about the magnetic properties of this alloy in the thin film state, which may impose specific compositional and structural limitations on the realization of antiferromagnetic ordering [5–8], which makes it difficult to correctly assess the potential of Cr-Mn films as a functional medium. This paper seeks to remedy this shortcoming to a certain extent by systematically studying the effect of design elements on the hysteresis properties of bilayer-based (Cr-Mn)/Fe film composites, and in a temperature section. The latter, on the one hand, reveals the specificity of the fundamental magnetic interactions in the studied objects and, on the other hand, provides direct information about the thermal sensitivity of important characteristics of functional materials, in particular those possessing an exchange shift effect.

2. Samples and procedures

The objects of the study were multilayer glass/X/(Cr-Mn)/Fe/Ta. They were produced by magnetron sputtering of single-component targets Ta, Fe, Cr, Mn, on Corning glass substrates. During the formation of the binary layer the co-spraying regime of Cr and Mn was applied, allowing the composition of this layer to be varied by changing the ratio of electrical powers on the targets. In addition, the thickness of the Cr-Mn layer and the composition of the buffer coating X, on which it was deposited, were varied. The buffer coating was a single layer and included only a 5 nm thick Ta layer or a double layer, in addition containing 5 nm thick Cr or Fe layers. The functions of the other elements of the film structure were summarized as follows. The 5 nm thick outer layer Ta played a protective role. The following 10 nm thick Fe layer was an indicator layer and carried the main information about the magnetic properties of the adjacent Cr-Mn layer. The entire film structure was formed under conditions of high-frequency electrical displacement of the substrate and the presence of a homogeneous magnetic field in its plane (process field) with a strength of 250 Oe.

A Nanohunter X-ray fluorescence spectrometer and a PANalytical Empyrean X-ray diffractometer were used to determine the composition of the Cr-Mn layer and to certify its structural state, respectively, in Co K_α. The magnetic property test consisted of measuring hysteresis loops in the plane of the film samples along the axis of the process field (longitudinal loops) application and perpendicular to this axis (transverse loops). In fact, these loops reflected the magnetic hysteresis in the Fe layer(s) present in all samples. The magnetic tests involved the EvicoMagnetics

Kerr magnetometer and the MPMS EverCool and PPMS DynaCool measuring systems from Quantum Design.

3. Discussion of results

In general, three ways of varying their design were used to obtain information about the features of magnetic hysteresis in the studied film structures: changing the ratio of components in layer Cr-Mn in the range of 10 to 80 at.% Mn; changing the thickness of this layer L (20 or 100 nm) and changing the buffer coating (Ta, Ta/Cr, Ta/Fe). It was assumed that thickness and buffer coating could affect the microstructure of the films by changing the size of Cr-Mn crystallites or the texture degree. In the latter case, it was taken into account that these metals, like the Cr-Mn alloy, have a body-centered cubic structure but differ in the lattice parameter a — 0.331; 0.289; 0.287 nm for Ta, Cr and Fe, respectively. Thus, the presence of a buffer will be reflected in the realization of an epitaxial build-up effect, which is often present in the formation of multilayer film structures [9]. In addition, it should be noted that Ta can also have a tetragonal lattice (α-Ta) [10]. However, β-Ta, as opposed to the volume-centered modification (α-Ta), is a metastable structure [11,12]. Therefore, the implementation of α-Ta in a buffer layer, despite its small thickness, seems more likely.

3.1. Hysteresis properties of films with Cr-Mn layers of different composition

Fig. 1 shows the dependences of the longitudinal coercive force H_c (determined from longitudinal magnetometric hysteresis loops) on temperature T for glass/Ta/$Cr_{100-x}Mn_x$(20)/Fe/Ta with $L = 20$ nm (indicated in brackets). As you can see, all $H_c(T)$ curves can be divided in two types. Some (curves *1, 2*) show a gradual increase in coercive force when decreasing T throughout the temperature range 5−300 K used, others (curves *3, 4*) show a sharp increase at $T < 100$ K. And for the temperature area $T > 100$ K the coercive force values in these curves are much lower than in the dependencies of the first kind, and they differ little from the level of H_c of iron film (glass/Ta/Fe/Ta), indicated by the dashed line in Fig. 1.

The data presented can be interpreted based on the position that the coercive force value of the Fe layer reflects not only its own magnetic hysteresis but also the hysteresis due to its interaction with the Cr-Mn layer. If the latter is in a disordered magnetic state, its contribution to H_c is minimal. In the opposite case, it significantly increases the coercive force of the adjacent ferromagnetic layer [13] due to its crystallites (all or part) exchanged with the ferromagnetic layer having a comparatively low magnetic anisotropy. Such crystallites do not provide an exchange displacement effect, but only impede the remagnetization of the ferromagnetic layer, eventually switching with it. With respect to our results, this may imply that the $20 \le x \le 40$ area is characterized by the antiferromagnetic state of the $Cr_{100-x}Mn_x$ layer over the whole temperature area in question. It is characterized by low magnetic anisotropy, as no marked anisotropy of the hysteresis properties is observed in the sample plane. With an Mn content of more than 40 at.% antiferromagnetizm is only realized at low temperatures.

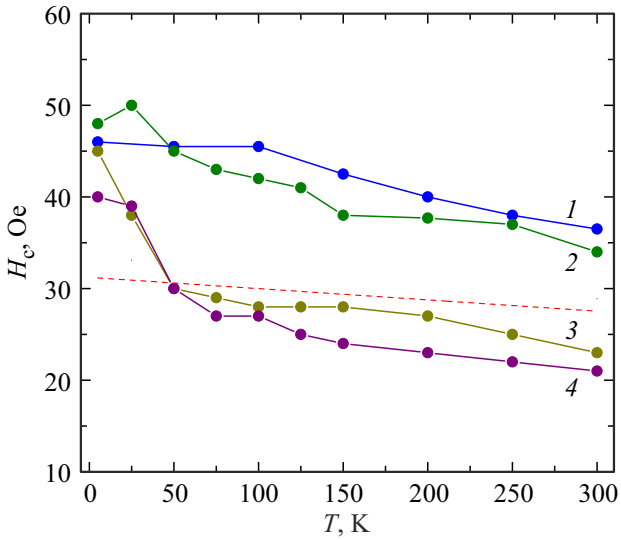

Figure 1. Temperature dependences of coercive force of glass/Ta/$Cr_{100-x}Mn_x$(20 nm)/Fe(10 nm)/Ta samples with Cr-Mn layers of different composition: *1* — 20; *2* — 40; *3* — 60; *4* — 80 at.% Mn. The dashed line shows the coercive force level of the Ta/Fe(10 nm)/Ta film.

3.2. Hysteresis properties and structure of films with different buffer coatings

Some modification of the hysteresis effect from interlayer exchange coupling can be expected by influencing the texture of the antiferromagnetic layer via buffer coatings. Fig. 2, *a* shows temperature dependences of coercive force for glass/X/$Cr_{80}Mn_{20}$(20 nm)/Fe(10 nm)/Ta samples with fixed Cr-Mn layer composition from antiferromagnetic state realization area and different variants of buffer coatings. It can be seen that all these dependences have approximately the same course and show a smooth and gentle increase in Hc with decreasing temperature, which can be attributed to an increase in magnetic anisotropy of both the Fe layer itself and the Cr-M layer. At the same time, there is a large difference in H_c levels for films with different buffer layers. The coercive force is higher when the crystal lattice parameters of the coating (Cr, Fe) and the Cr-Mn layer are close. This shows that the effect of varying the buffer layer composition does occur and probably reflects certain changes in the microstructure of the films.

Fig. 2, *b* shows diffraction patterns of the same samples. The lines appearing on them are most likely formed by Cr-Mn and Fe layers, which are the thickest and have

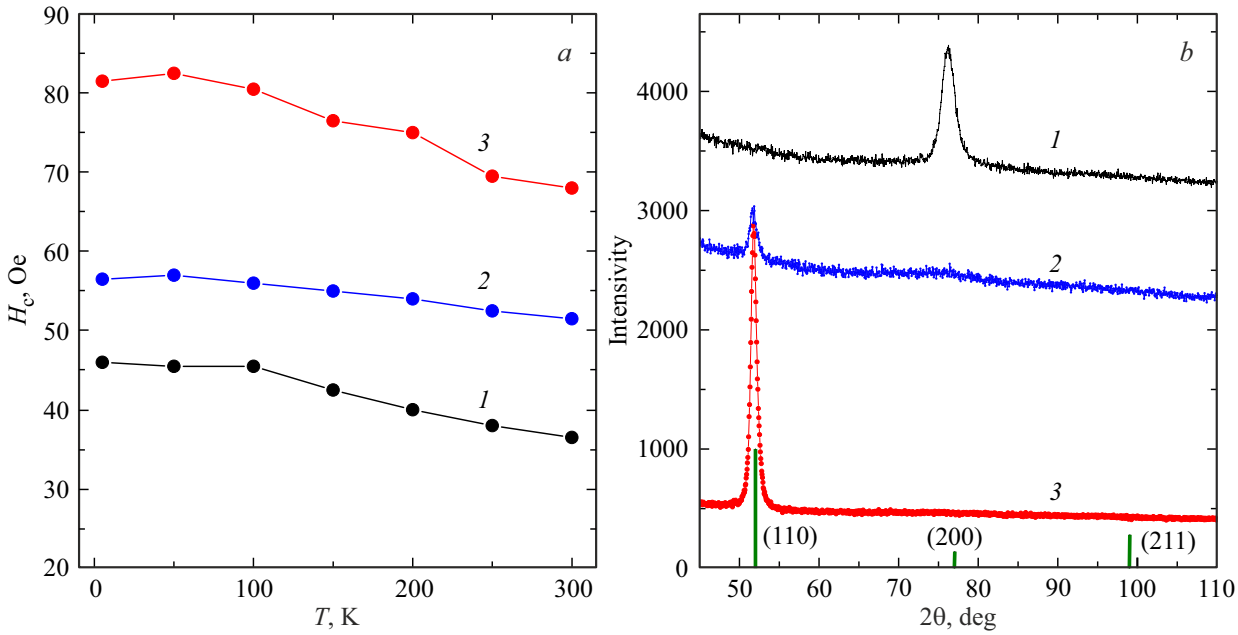

Figure 2. Temperature dependences of coercive force (a) and diffraction patterns (b) of glass/X/$Cr_{80}Mn_{20}$(20 nm)/Fe(10 nm)/Ta samples with different buffer coatings X: *1* — Ta; *2* — Ta/Cr; *3* — Ta/Fe. The vertical bars indicate the calculated position and ratio of the diffraction line intensities of polycrystalline untextured Cr.

close lattice parameters. These, as well as the rocking curves additionally measured near these lines, show that a crystalline texture is present in all the films, and a different one at that. On the Ta cover, it is of type (200), and on the other two covers — it is of type (110). This correlates in some ways with the data on hysteresis properties. From the above results, it can be concluded that a texture of type (110) corresponds to an increased H_c. Ta/Fe coating appears to have the most pronounced texture, and consequently the coercive force of this film is the greatest. This feature can presumably be attributed to an increase in the exchange efficiency at the (Cr-Mn)/Fe interface, when the lattices of the two layers are coupled like (110), consisting of more antiferromagnetic crystallites being involved in the switching.

3.3. Influence of Cr-Mn layer thickness on hysteresis properties of films

The results presented above indirectly indicate an antiferromagnetic ordering in the Cr-Mn layer and even to a certain extent indicate the concentration and temperature ranges of its realization. At the same time, none of the examined samples showed an exchange shift, i.e. a shift of the hysteresis loop of the Fe layer along the magnetic field axis, the presence of which can be considered as unequivocal evidence of ferro/antiferromagnetic exchange coupling. In all cases, there was a complete absence of hysteresis anisotropy in the plane. A probable reason for this may be the low anisotropy constant of the material and the correspondingly low magnetic anisotropy energy of the individual crystallites, which determines their resistance to switching under the influence of the exchange bond with the ferromagnetic layer. The natural way to enhance it is to increase the volume of crystallites. For this purpose, films with thicker Cr-Mn layers (100 nm) were used in the expectation that an increase in thickness would result in an increase in the average crystallite size.

Fig. 3 shows examples of magneto-optical hysteresis loops of glass/Ta/$Cr_{80}Mn_{20}$(L)/Fe/Ta with $L = 20$ and 100 nm for comparison, including those measured along and across the process field axis. Indeed, they significantly differ in both qualitative and quantitative terms. Firstly, an exchange displacement effect (curve *1* in Fig. 3, b) appeared in the films with $L = 100$ nm, i.e. unidirectional anisotropy appeared. The consequence is the difference in the longitudinal (curve 1) and transverse (curve 2) loops, which is completely absent in the sample with $L = 20$ (Fig. 3, a). Secondly, as the thickness of the Cr-Mn layer increased, the coercive force increased. Whereas in free Fe film at room temperature, it was about 25 Oe, in the sample with $L = 20$, it reached 45 Oe, and it was at $L = 100-65$ Oe.

Fig. 3, c shows the temperature dependences of the main hysteresis characteristics of film glass/Ta/$Cr_{80}Mn_{20}$(100 nm)/Fe/Ta to which the longitudinal loop coercive force H_c, the difference between the longitudinal and transverse loop coercive forces ΔH_c and the absolute value of exchange displacement field $|H_{ex}|$ are referenced. As can be seen, $H_c(T)$ and $\Delta H_c(T)$ dependences are very similar, which allows to associate the low-temperature increase in magnetic hysteresis primarily with an increase in the magnetic anisotropy constant of the antiferromagnetic.

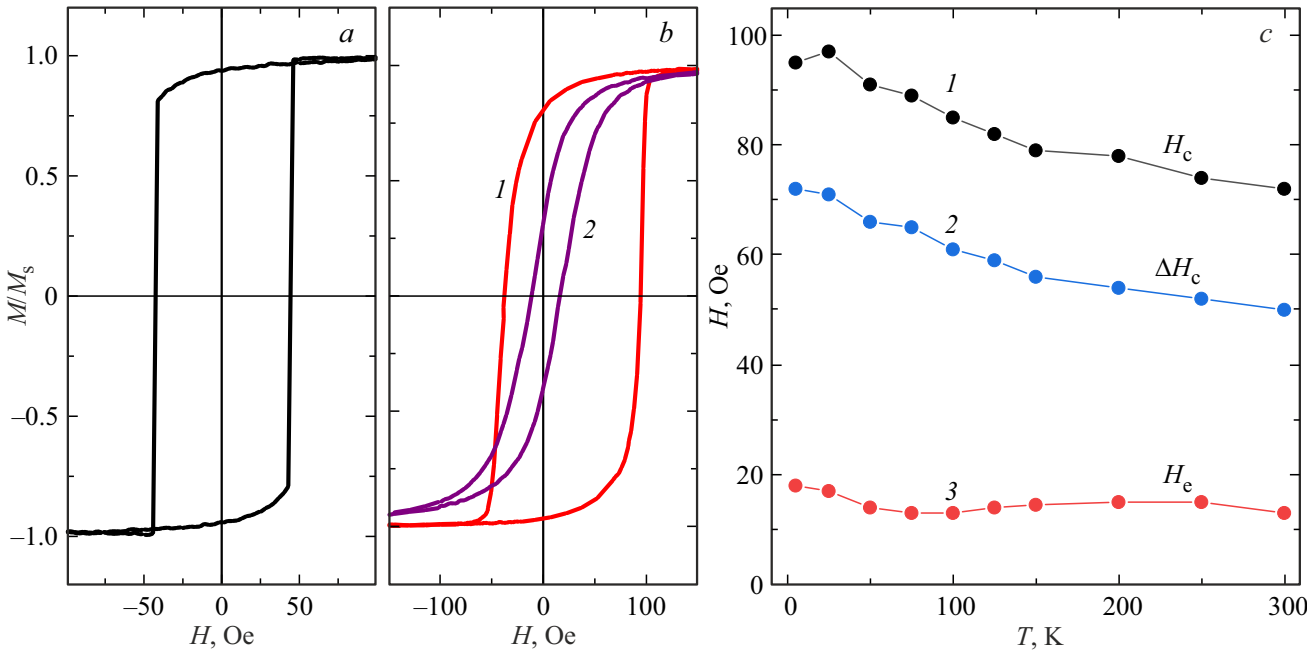

Figure 3. Hysteresis loops (a, b) and temperature dependences of hysteresis properties of films (c) glass/Ta/$Cr_{80}Mn_{20}$(L)/Fe/Ta with $L = 20$ (a) and 100 nm (b, c). Numbers *1* and *2* in figure *b* denote the longitudinal and transverse loops, respectively. In Fig. *c*, the numbers *1*, *2* and *3* correspond to the values H_c, ΔH_c, $|H_{ex}|$.

However, the exchange displacement field does not undergo significant temperature changes, thus indirectly showing that the number of stable antiferromagnetic crystallites practically does not increase with decreasing temperature. It should also be noted that, according to X-ray analysis, there is no crystalline texture in this sample. All this data leads to the following conclusions. Firstly, the significant difference in crystal lattice parameters has a negative effect on texture formation in mating layers as they increase in thickness. Secondly, the presence of a crystalline texture is not a prerequisite for the formation of an exchange displacement.

The sample with $L = 100$ nm on the Ta/Cr buffer coating is slightly different. The value of its $H_c(T)$ is weakly temperature dependent but generally has a higher level (~ 110 Oe) than the film at Ta. In contrast, the value of $|H_{ex}|$ increases as the temperature decreases in the range 300–5 K from 10 to almost 30 Oe. Characteristically, the crystalline texture of type (110) inherent in the thin film on the Ta/Cr coating is retained even with the large thickness of the antiferromagnetic layer. This suggests that the presence of texture modifies the size distribution of the antiferromagnetic crystallites in some way and they are in a near-stable state. Temperature lowering initiates magnetic stabilization of the crystallites and forms dependence $|H_{ex}|(T)$ through a series of transitions across local locking temperatures.

Sample $L = 100$ nm on the Ta/Fe buffer coating also showed its own specific hysteresis properties when varying the temperature. In it, just as in the Ta/Cr film, the crystal texture of type (110) was preserved with increasing thickness, but the presence of ferromagnetic layers at both interfaces of the Cr-Mn layer changed the remagnetization conditions of the whole structure. Fig. 4, *a* shows the magneto-optical loops measured at room temperature on both sides of the sample glass/Ta/F(5 nm)/$Cr_{80}Mn_{20}$(100 nm)/Fe(10 nm)/Ta. They reflect the remagnetization of the main (10 nm thick) and the buffer (5 nm thick) Fe layers, which are seen to differ greatly in coercive force. And the high H_c is inherent in the thicker layer, which is unlikely to be the case with free remagnetization. Presumably, this can be related to the heterogeneous thickness of the Cr-Mn microstructure, namely the larger average crystallite size at the upper interface, and hence a stronger anchoring of the main ferromagnetic layer.

Attention should also be paid to the exchange displacement of both layers Fe. Although small, it is confidently fixable. And the exchange bond field of the buffer layer is slightly larger (7.5 Oe) than that of the main layer (5 Oe). However, this should not be seen as evidence of a more effective effect on the thin layer by the antiferromagnetic. Simply, the small thickness provides less pressure on the magnetic moment from the external magnetic field and results in a higher value H_{ex}. This is shown by assessments made using the well-known formula [14,15]:

$$H_{ex} = \frac{K_s}{M_s h}, \qquad (1)$$

where M_s — spontaneous iron magnetization (1700 G), h — ferromagnetic layer thickness, K_s — phenomenological

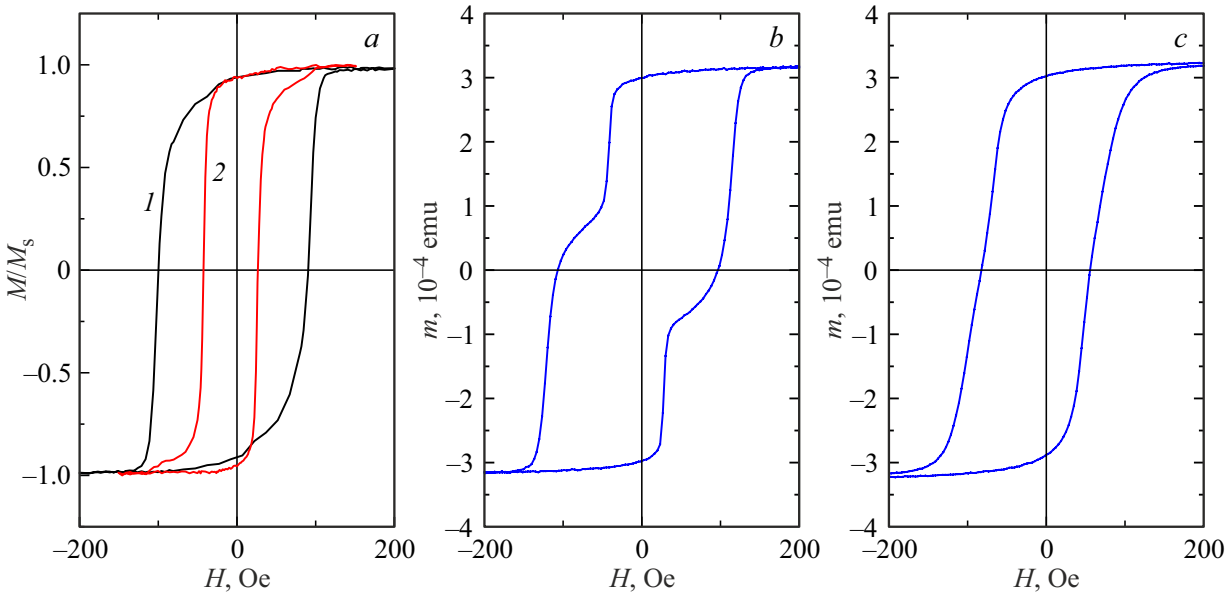

Figure 4. Magneto-optical (a) and magnetometric (b, c) hysteresis loops measured on glass/Ta/F(5 nm)/$Cr_{80}Mn_{20}$(100 nm)/Fe(10 nm)/Ta. Numbers *1* and *2* denote the loops of the main (thickness 10 nm) and buffer (thickness 5 nm) Fe layers, respectively.

constant of interlayer exchange coupling. K_s values calculated using the above formula for layers 10 and 5 nm thick are $85 \cdot 10^{-4}$ and $65 \cdot 10^{-4}$ erg/cm ^{2}, respectively. That is, the exchange coupling at the lower interface of the antiferromagnetic layer is indeed weaker than at the upper one. And in both cases, it is considerably inferior in order of magnitude to the Fe−Mn/Fe type structure, for which K_s is $340 \cdot 10^{-4}$ erg/cm ^{2} [16].

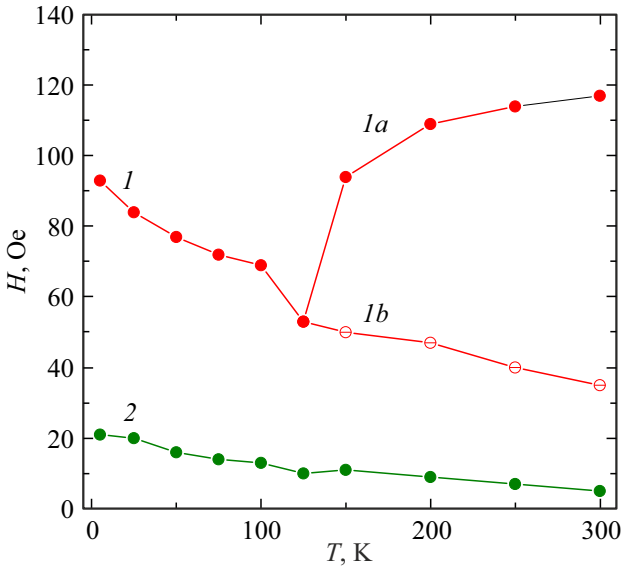

Figure 5. Temperature dependences of the longitudinal coercive force (curves *1*) and exchange displacement field (curve *2*) in sample glass/Ta/F(5 nm)/$Cr_{80}Mn_{20}$(100 nm)/Fe(10 nm)/Ta. Parts of the $H_c(T)$ dependence relate to the main (*1 a*) and buffer (*1 b*) layers Fe, and the dependence $H_{ex}(T)$ — to the main layer.

Interestingly, the relative independence in the remagnetization of the Fe layers disappears with decreasing temperature. This can be seen by comparing the magnetometric hysteresis loops, also shown in Fig. 4. At room temperature (Fig. 4, b), the loop is stepped, describing layer-by-layer remagnetization, and near 100 K (Fig. 4, c), it takes the usual form, indicating joint remagnetization of the layers. A general picture of the temperature behavior of the hysteresis characteristics in the glass/Ta/F(5 nm)/$Cr_{80}Mn_{20}$(100 nm)/Fe(10 nm)/Ta sample can be drawn from Fig. 5. As can be seen, the coercive force of the buffer layer increases monotonically with decreasing temperature and is much stronger than in samples with other buffer coatings. The dependence of $H_c(T)$ of the main layer shows a sharply non-monotone course, experiencing a dip around $T \sim 120$ K. Near this temperature, the remagnetization of the two layers merges into a single process. This can be regarded as indirect evidence of strengthening the effective exchange interaction within the antiferromagnetic layer (also due to the temperature blocking of small crystallites), preventing the formation of a non-uniform magnetization distribution over the entire sample thickness.

4. Conclusion

This study shows that the system Cr-Mn in the film state in a sufficiently wide range of compositions and temperatures exhibits antiferromagnetic properties, which layers can exert magnetic clamping effect on the adjacent layers Fe. The effectiveness of this action depends primarily on the antiferromagnetic layer thickness, and if it is thick

enough (~ 100 nm) varies in a certain way depending on the material of the buffer layers. This includes situations where the coercive force monotonically increases with decreasing temperature or changes non-monotonically, and the exchange displacement field also increases or reacts weakly to temperature changes. The most probable cause of the identified patterns is the change in average crystallite size with varying thickness and including the formation of a thickness dispersion in crystallite size. In addition, the formation of these patterns is influenced by changes in the crystal texture and the temperature change in the anisotropy constant of the antiferromagnetic.

Funding

This paper was supported financially by RSF (grant No. 22-22-00814.

Conflict of interest

The authors declare that they have no conflict of interest.

References

[1] S. Maki, K. Adachi. J. Phys. Soc. Jpn **46**, *4*, 1131 (1979).
[2] T. Blachowicz, A. Ehrmann. Coatings **11**, *2*, 122 (2021).
[3] K. O'Grady, J. Sinclair, K. Elphick, R. Carpenter, G. Vallejo-Fernandez, M.I.J. Probert, A. Hirohata. J. Appl. Phys. **128**, *4*, 040901 (2020).
[4] W.H. Meiklejohn, C.P. Bean. Phys. Rev. **105**, *3*, 904 (1957).
[5] W. Feng, J. Choi, D.D. Dung, S. Cho, X. Hao. J. Appl. Phys. **108**, *7*, 073915 (2010).
[6] J. Juraszek, J. Fassbender, S. Poppe, T. Mewes, B. Hillebrands, D. Engel, A. Kronenberger, A. Ehresmann, H. Schmoranzer. J. Appl. Phys. **91**, *10*, 6896 (2002).
[7] S. Soeya, H. Hosiya, M. Fuyama, S. Tadokoro. J. Appl. Phys. **80**, *2*, 1006 (1996).
[8] S. Soeya, H. Hosiya, R. Arai, M. Fuyama. J. Appl. Phys. **81**, *9*, 648 (1997).
[9] V.O. Vas'kovskiy, V.N. Lepalovskij, A.N. Gor'kovenko, N.A. Kulesh, P.A. Savin, A.V. Svalov, E.A. Stepanova, A.A. Yuvchenko, N.N. Shchegoleva. Tech. Phys. **60**, 116 (2015).
[10] A.A. Navid, A.M. Hodge. Mater. Sci. Eng. A **536**, 49 (2012).
[11] A. Jara, B. Fraisse, V. Flaud, N. Fréty, G. Gonzalez. Surf. Coatings Technol. **309**, 887 (2017).
[12] D. Bernoulli, U. Müller, M. Schwarzenberger, R. Hauert, R. Spolenak. Thin Solid Films **548**, 157 (2013).
[13] I. Žutić, J. Fabian, S.D. Sarma. Rev. Mod. Phys. **76**, *2*, 323 (2004).
[14] K. O'grady, L.E. Fernandez-Outon, G. Vallejo-Fernandez. J. Magn. Magn. Mater. **322**, *8*, 883 (2010).
[15] D. Mauri, E. Kay, D. Scholl, J.K. Howard. J. Appl. Phys. **62**, *7*, 2929 (1987).
[16] V.O. Vas'kovskiy, A.N. Gorkovenko, N.A. Kulesh, V.N. Lepalovskij, M.E. Moskalev. Thin Solid Films **764**, 139616 (2023).

Translated by Ego Translating